

Multiparticle azimuthal cumulants in $p + \text{Pb}$ collisions from a multiphase transport model

Mao-Wu Nie,^{1,2,3} Peng Huo,⁴ Jiangyong Jia,^{4,5} and Guo-Liang Ma^{1,*}

¹Shanghai Institute of Applied Physics, Chinese Academy of Sciences, Shanghai 201800, China

²University of Chinese Academy of Sciences, Beijing 100049, China

³Institute of Frontier and Interdisciplinary Science & Key Laboratory of Particle Physics and Particle Irradiation (MOE), Shandong University, Qingdao 266237, China

⁴Department of Chemistry, Stony Brook University, Stony Brook, New York 11794-3800, USA

⁵Physic Department, Brookhaven National Laboratory, Upton, New York 11796, USA



(Received 29 January 2018; published 4 September 2018)

A new subevent cumulant method was recently developed, which can significantly reduce the nonflow contributions in long-range correlations for small systems compared to the standard cumulant method. In this work, we study multiparticle cumulants in $p + \text{Pb}$ collisions at $\sqrt{s_{\text{NN}}} = 5.02$ TeV with a multiphase transport model (AMPT), including two- and four-particle cumulants ($c_2\{2\}$ and $c_2\{4\}$) and symmetric cumulants [SC(2, 3) and SC(2, 4)]. Our numerical results show that $v_2\{2\}$ is consistent with the experimental data, while the magnitude of $c_2\{4\}$ is smaller than the experimental data, which may indicate that either the collectivity is underestimated or some dynamical fluctuations are absent in the AMPT model. For the symmetric cumulants, we find that the results from the standard cumulant method are consistent with the experimental data, but those from the subevent cumulant method show different behaviors. The results indicate that the measurements from the standard cumulant method are contaminated by nonflow effects, especially when the number of produced particles is small. The subevent cumulant method is a better tool to explore the *real* collectivity in small systems.

DOI: [10.1103/PhysRevC.98.034903](https://doi.org/10.1103/PhysRevC.98.034903)

I. INTRODUCTION

One experimental signature suggesting the formation of nearly perfect fluid in ultrarelativistic nucleus-nucleus (A+A) collisions is the azimuthal anisotropy of produced particles. The measured anisotropies provide strong evidence of collective flow, which is commonly believed to be related to the hot QCD medium that expands collectively and transfers asymmetries in the initial geometry space into azimuthal anisotropies of produced particles in the final momentum space [1–6]. The feature of collectivity appears in the form of a “ridge”: enhanced pair production in a small azimuthal angle interval, $\Delta\phi \sim 0$, extended over a wide range of pseudorapidity intervals $\Delta\eta$ [7–10]. The azimuthal structure of the ridge is typically analyzed via a Fourier decomposition, $dN_{\text{pairs}}/d\Delta\phi \sim 1 + 2 \sum v_n^2 \cos(n\Delta\phi)$. The second (elliptic; v_2) and third (triangular; v_3) Fourier harmonics are under intensive study, because they are assumed to directly reflect the medium response to the initial geometry. For a small collision system, such as proton-proton ($p + p$) or proton-nucleus ($p + \text{A}$) collisions, it was assumed that the transverse size of the produced system is too small compared to the mean free

path of constituents. Thus, it was expected that the collective flow in small systems should be much weaker than that in A+A collisions. However, recent observations of large long-range ridgelike correlations and v_n coefficients in small systems [11–17] challenge the above paradigm of collective flow.

Since hydrodynamic flow implies a global collectivity involving all particles in the event, k -particle azimuthal cumulants, $c_n\{k\}$, are often used to measure the *true* v_n [18,19]. The standard cumulant method, known as the Q -cumulant [19], uses all k -particle multiplets in the entire detector acceptance to calculate $c_n\{k\}$. But this method can be contaminated by nonflow effects, like jetlike correlation, especially when the multiplicity is low. Recently an improved cumulant method, referred to as the “subevent cumulant,” in which particles are divided into different subevents separated in the pseudorapidity η direction, was developed [20]. Compared to the standard cumulant method, the new method can more effectively suppress intrajet (single-jet) and interjet (dijet) correlations. Recent ATLAS measurements have shown that the subevent method provides a more precise determination of $c_n\{4\}$ associated with long-range collectivity in small systems [21].

Multiparticle correlation between different orders of flow harmonics is another complementary observable which provides additional constraints on the medium properties [22,23]. Such mixed-harmonic correlations are measured through the so-called symmetric cumulant, $\text{SC}(n, m)$, with $n \neq m$. The CMS Collaboration recently obtained results for SC(2, 3) and SC(2, 4) in $p + p$ and $p + \text{Pb}$ collisions based on the standard cumulant method [24]. However, Huo *et al.* argued that the measurements of $\text{SC}(n, m)$ in small systems are not trustworthy due to dominating nonflow effects, unless the subevent method

*glma@sinap.ac.cn

Published by the American Physical Society under the terms of the [Creative Commons Attribution 4.0 International](https://creativecommons.org/licenses/by/4.0/) license. Further distribution of this work must maintain attribution to the author(s) and the published article’s title, journal citation, and DOI. Funded by SCOAP³.

is utilized [25]. But their argument is based on the PYTHIA and HIJING models, which have no collective flow. Therefore it is necessary to verify this assertion with models that contain both collective flow and nonflow.

Two classes of theoretical scenarios have been proposed to explain the collectivity in small systems: hydrodynamical (or transport) models, which respond to the initial geometry through final-state interactions [26–36]; and the color glass condensate framework, which reflects the initial momentum correlation from gluon saturation effects [37–44]. Both scenarios can describe the current experimental results. For example, a multiphase transport (AMPT) model with a tuned elastic parton-parton cross section $\sigma = 3$ mb can naturally reproduce the long-range two-particle azimuthal correlation and two-particle v_n in high-multiplicity $p + \text{Pb}$ and $p + p$ collisions and show good agreement with the experimental data [31,32]. However, the collectivity from the AMPT model has been interpreted as a parton escape mechanism where the azimuthal anisotropy is mainly generated by anisotropic parton escape instead of hydrolike interactions [45,46]. The controversy surrounding the origin of collectivity in small systems needs to be further tested in more experimental and theoretical efforts.

In this work, we adopt the newly developed subevent cumulant method to suppress nonflow effects to investigate the flow in the AMPT model for $p + \text{Pb}$ collisions at $\sqrt{s_{NN}} = 5.02$ TeV. The two- and four-particle azimuthal cumulants ($c_2\{2\}$ and $c_2\{4\}$) and multiparticle azimuthal correlations between v_2 and v_3 and between v_2 and v_4 [SC(2, 3) and SC(2, 4)] are calculated using both standard and subevent cumulant methods. We find that the AMPT model can well describe the two-particle $v_2\{2\}$ data, but with a magnitude of $c_2\{4\}$ smaller than the experimental data. To further shed light on the origin and evolution of multiparticle correlations, the evolution of $c_2\{k\}$ values is traced at different phases in the AMPT model. Significant differences in symmetric cumulants, SC(2, 3) and SC(2, 4), between the standard and the subevent cumulant methods are also observed. Our results suggest that either the collectivity is underestimated or some non-Gaussian dynamical fluctuations are missing in the AMPT model. We find that the subevent cumulant method is a better probe to investigate the *real* collectivity in small systems.

II. THE AMPT MODEL

A multiphase transport model [47], which is a hybrid dynamical transport model, is utilized in this work. We use the string-melting AMPT version to simulate $p + \text{Pb}$ collisions at $\sqrt{s_{NN}} = 5.02$ TeV. The string-melting version consists of four main components: fluctuating initial conditions from the HIJING model [48], elastic parton cascade simulated by the ZPC model [49] for all partons from the melting of hadronic strings, a quark coalescence model for hadronization, and hadron rescatterings described by the ART model [50]. For details, see the review [47]. For the setting of parameter values, we follow the recent AMPT study with a modest elastic parton-parton cross section $\sigma = 3$ mb, which has been shown to be capable of reproducing the long-range correlation and

two-particle v_n coefficients in $p + \text{Pb}$ collisions at $\sqrt{s_{NN}} = 5.02$ TeV [31,32].

III. MULTIPARTICLE CUMULANTS

The cumulant method has been developed to characterize multiparticle correlations related to the collective expansion of system, while reducing nonflow contributions order by order [18,51]. A $2k$ -particle azimuthal correlator $\langle\langle 2k \rangle\rangle$ is obtained by averaging over all unique combinations in one event, then over all events, where the first two terms are $\langle\langle 2 \rangle\rangle = \langle\langle e^{in(\phi_1 - \phi_2)} \rangle\rangle$ and $\langle\langle 4 \rangle\rangle = \langle\langle e^{in(\phi_1 + \phi_2 - \phi_3 - \phi_4)} \rangle\rangle$. For a given harmonic n , the two- and four-particle cumulants can be determined:

$$c_n\{2\} = \langle\langle 2 \rangle\rangle, \quad (1)$$

$$c_n\{4\} = \langle\langle 4 \rangle\rangle - 2\langle\langle 2 \rangle\rangle^2. \quad (2)$$

The flow coefficients v_n can be analytically obtained from the two- and four-particle cumulants:

$$v_n\{2\} = \sqrt{c_2\{2\}}, \quad (3)$$

$$v_n\{4\} = \sqrt[4]{-c_n\{4\}}. \quad (4)$$

The framework of the standard cumulant [19] expresses multiparticle correlations in terms of powers of the flow vector $Q_n = \sum e^{in\phi}$. The multiparticle correlations and cumulants can be calculated through a single loop over all events. In the standard cumulant method, the particles are chosen from the entire detector acceptance. In small systems, the nonflow correlations, especially the jet and dijet, dominate the azimuthal correlations. Hence, the standard cumulant may be strongly biased by these nonflow correlations, while the subevent cumulant method is designed to further suppress these nonflow correlations. In the subevent cumulant method, the entire event is divided into two subevents or three subevents. Specifically, in the two-subevent method, the event is divided into two (labeled a and b) according to $-\eta_{\max} < \eta_a < 0$ and $0 < \eta_b < \eta_{\max}$; in the three-subevent method, the event is divided into three (labeled a , b , and c) according to $-\eta_{\max} < \eta_a < -\eta_{\max}/3$, $-\eta_{\max}/3 < \eta_b < \eta_{\max}/3$, and $\eta_{\max}/3 < \eta_c < \eta_{\max}$. Then one can get the $2k$ -particle azimuthal correlators as follows:

$$\langle\langle 2 \rangle\rangle_{\text{two-sub}} = \langle\langle e^{in(\phi_1^a - \phi_2^b)} \rangle\rangle, \quad (5)$$

$$\langle\langle 4 \rangle\rangle_{\text{two-sub}} = \langle\langle e^{in(\phi_1^a + \phi_2^a - \phi_3^b - \phi_4^b)} \rangle\rangle, \quad (6)$$

$$\langle\langle 4 \rangle\rangle_{\text{three-sub}} = \langle\langle e^{in(\phi_1^a + \phi_2^a - \phi_3^b - \phi_4^c)} \rangle\rangle. \quad (7)$$

The symmetric cumulant is also based on the multiparticle cumulants, which measure the correlation between different flow harmonics on the basis of event-by-event fluctuations. The SC(n , m) is defined below:

$$\begin{aligned} \text{SC}(n, m) &= \langle\langle e^{in(\phi_1 - \phi_2) + im(\phi_3 - \phi_4)} \rangle\rangle - \langle\langle e^{in(\phi_1 - \phi_2)} \rangle\rangle \langle\langle e^{im(\phi_3 - \phi_4)} \rangle\rangle \\ &= \langle v_m^2 v_n^2 \rangle - \langle v_m^2 \rangle \langle v_n^2 \rangle. \end{aligned} \quad (8)$$

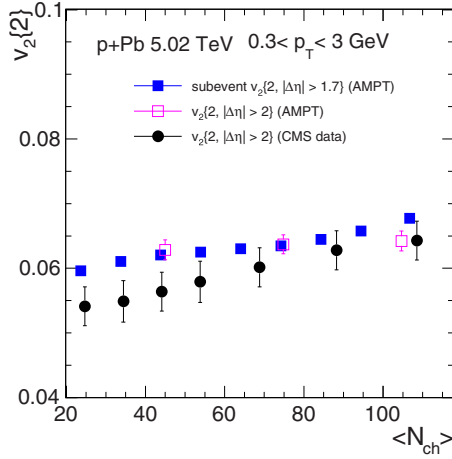


FIG. 1. $v_2\{2\}$ as a function of the number of charge particles ($\langle N_{\text{ch}} \rangle$) in $p + \text{Pb}$ collisions at $\sqrt{s_{\text{NN}}} = 5.02$ TeV, where filled squares represent the AMPT results using the subevent method, while open squares and filled circles represent the two-particle correlation results (with $|\Delta\eta| > 2$) from the published AMPT results [32] and CMS data [52], respectively.

Similarly, we can easily get the $\text{SC}(n, m)$ with the subevent methods,

$$\text{SC}(n, m)_{\text{two-sub}} = \left\langle \left\langle e^{in(\phi_1^a - \phi_2^b) + im(\phi_3^a - \phi_4^b)} \right\rangle \right\rangle - \left\langle \left\langle e^{in(\phi_1^a - \phi_2^b)} \right\rangle \right\rangle \left\langle \left\langle e^{im(\phi_3^a - \phi_4^b)} \right\rangle \right\rangle, \quad (9)$$

$$\text{SC}(n, m)_{\text{three-sub}} = \left\langle \left\langle e^{in(\phi_1^a - \phi_2^b) + im(\phi_3^a - \phi_4^c)} \right\rangle \right\rangle - \left\langle \left\langle e^{in(\phi_1^a - \phi_2^b)} \right\rangle \right\rangle \left\langle \left\langle e^{im(\phi_3^a - \phi_4^c)} \right\rangle \right\rangle. \quad (10)$$

More details can be found in Ref. [20].

In order to make our results directly comparable to the experimental measurements, we choose $\eta_{\text{max}} = 2.5$ in our analysis to mimic the ATLAS detector acceptance for charged particles. The event selection is based on $\langle N_{\text{ch}} \rangle$, the number of charged particles in $|\eta| < 2.5$, and $p_T > 0.4$ GeV. The cumulant calculations are carried out using the charge particles in $|\eta| < 2.5$ and a certain p_T selection, $0.3 < p_T < 3$ GeV, and the number of charged particles in this p_T range, $N_{\text{ch}}^{\text{sel}}$. We need to point out that $N_{\text{ch}}^{\text{sel}}$ and N_{ch} are not the same due to different p_T ranges. Then $\langle 2k \rangle$ is averaged over events with the same $N_{\text{ch}}^{\text{sel}}$ to obtain the $\langle \langle 2k \rangle \rangle$ and $\text{SC}(n, m)$. Finally, the cumulant results are obtained by mapping $N_{\text{ch}}^{\text{sel}}$ to $\langle N_{\text{ch}} \rangle$, where we follow the ATLAS procedure exactly with the same kinematic cuts [21].

IV. RESULTS AND DISCUSSION

Figure 1 shows the $v_2\{2\}$ results with the subevent cumulant method and compares them with the two-particle $v_2\{2, |\Delta\eta| > 2\}$ from the published AMPT results [32] and the CMS data [52]. The three results are in good agreement.

Figure 2 shows the $c_2\{4\}$ results as a function of the number of charge particles, where the AMPT results are calculated with three methods (standard cumulant, two-subevent cumulant, and three-subevent cumulant methods), in comparison with

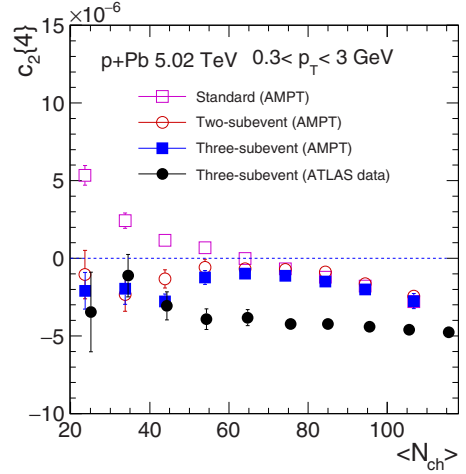


FIG. 2. $c_2\{4\}$ as a function of the number of charge particles ($\langle N_{\text{ch}} \rangle$) in $p + \text{Pb}$ collisions at $\sqrt{s_{\text{NN}}} = 5.02$ TeV, where open squares, open circles, and filled squares represent the AMPT results using the standard cumulant, two-subevent, and three-subevent methods, respectively. Filled circles represent the ATLAS data using the three-subevent cumulant method [21].

the experimental data. We find that $c_2\{4\}$ using the standard cumulant method is negative at $\langle N_{\text{ch}} \rangle > 70$ but changes to positive at $\langle N_{\text{ch}} \rangle < 70$, a region expected to be more affected by nonflow contributions. In contrast to the standard cumulant method, the $c_2\{4\}$ from subevent methods remains negative over the full $\langle N_{\text{ch}} \rangle$ region. It is surprising that the $c_2\{4\}$ using the two-subevent method agrees almost completely with that using the three-subevent method. This may indicate that the two-subevent method already suppresses most of the nonflow contributions in the AMPT model. On the other hand, the magnitude of $c_2\{4\}$ with the AMPT model is systematically smaller than that with the ATLAS data. Since $c_2\{4\}$ is sensitive to not only the averaged collectivity (v_2) but also the shape of the v_2 probability distribution $p(v_2)$ [53–55], the lack of $c_2\{4\}$ may indicate that either the collectivity is underestimated or some non-Gaussian dynamical fluctuations of v_2 are missing in the AMPT model [56].

To further investigate the collectivity behavior, we trace the values of $c_2\{2\}$ and $c_2\{4\}$ at four evolution stages: initial stage, after parton cascade, after coalescence, and after hadronic rescatterings. The $c_2\{2\}$ and $c_2\{4\}$ at these four stages are all calculated using the three-subevent method, as shown in Figs. 3 and 4, respectively. At the initial stage, the $c_2\{2\}$ and $c_2\{4\}$ are slightly positive at small $\langle N_{\text{ch}} \rangle$ and asymptotically approach 0 towards larger $\langle N_{\text{ch}} \rangle$. This behavior is consistent with the expectation from transverse momentum conservation [57]. After parton cascade, $c_2\{2\}$ is enhanced and $c_2\{4\}$ changes sign from positive to negative at a certain value of $\langle N_{\text{ch}} \rangle$, which may be due to the interplay between transverse momentum conservation and an anisotropic flow generated by parton cascade [58]. After coalescence, the more positive $c_2\{2\}$ and more negative $c_2\{4\}$ are seen for all charged hadrons not including resonances, which indicates that the strength of collective correlations increases, since both $\langle p_T \rangle$ and $v_2(p_T)$ can be enhanced via the coalescence process. In the final stage, i.e.,

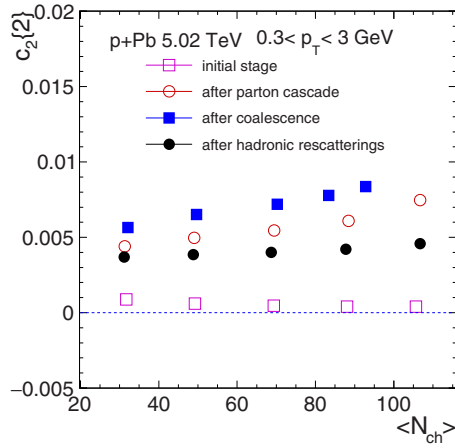


FIG. 3. AMPT results on $c_2\{2\}$ with the three-subevent method as a function of the number of charge particles $\langle N_{ch} \rangle$ for four evolution stages, i.e., initial stage (open squares), after parton cascade (open circles), after coalescence (filled squares), and after hadronic rescatterings (filled circles), in $p + \text{Pb}$ collisions at $\sqrt{s_{NN}} = 5.02$ TeV.

after hadronic rescatterings, the magnitudes of $c_2\{2\}$ and $c_2\{4\}$ decrease significantly because of the cooling-down of systems. However, we note that hadronic rescatterings suppress $c_2\{4\}$ more strongly than $c_2\{2\}$ (by a factor of ~ 8 vs 2); the detailed dynamics of this behavior deserves further investigation in the future.

Figures 5 and 6 show the symmetric cumulants $SC(2, 3)$ and $SC(2, 4)$, respectively. The results using three methods are presented (standard cumulant, two-subevent cumulant, and three-subevent cumulant methods), in comparison with the CMS data, which are based on the standard cumulant method. We find that the $SC(2, 3)$ from the standard cumulant method is negative at a high multiplicity, while it becomes positive at a low multiplicity, which is in good agreement with the CMS data. However, we find that the $SC(2, 3)$ from the subevent methods stays negative for the whole range of multiplicities. Our results strongly suggest that the measurements using

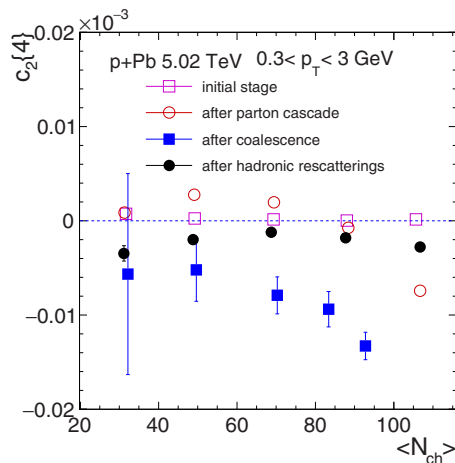


FIG. 4. Same as Fig. 3, but for $c_2\{4\}$ with the three-subevent method.

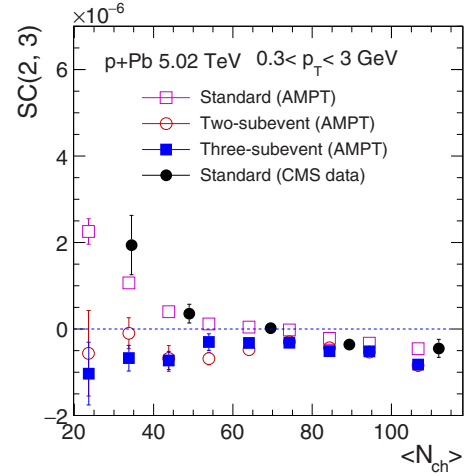


FIG. 5. $SC(2, 3)$ as a function of the number of charge particles $\langle N_{ch} \rangle$ from AMPT calculations using the standard cumulant (open squares), two-subevent (open circles), and three-subevent (filled squares) methods, in comparison with the experimental data with the standard cumulant method (filled circles) [24], in $p + \text{Pb}$ collisions at $\sqrt{s_{NN}} = 5.02$ TeV.

the standard cumulant method are contaminated by nonflow effects. On the other hand, the $SC(2, 4)$ from the standard cumulant method is comparable with the experimental data, but it is much larger than those with subevent methods. It also suggests that nonflow contributions need to be removed to obtain a clean signal of collectivity, especially in the low-multiplicity region in small systems.

V. CONCLUSIONS

The subevent cumulant method is utilized to study multiparticle correlations in $p + \text{Pb}$ collisions within the AMPT model. The two- and four-particle cumulants ($c_2\{2\}$ and $c_2\{4\}$) and multiparticle azimuthal correlations between different flow harmonics [$SC(2, 3)$ and $SC(2, 4)$] are numerically calculated. $v_2\{2\}$ is consistent with the experimental data, while the

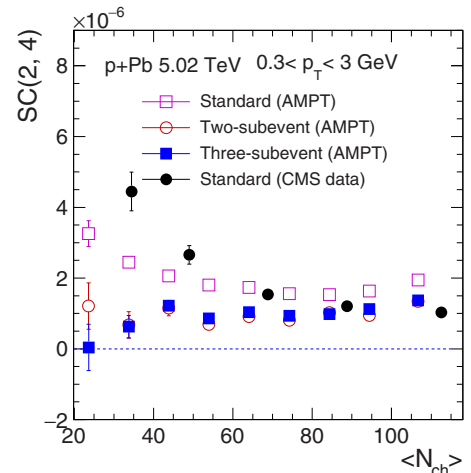


FIG. 6. Same as Fig. 5, but for $SC(2, 4)$.

magnitude of $c_2\{4\}$ is systematically smaller than the experimental data. This behavior indicates that either the collectivity is underestimated or some non-Gaussian dynamical fluctuations are absent in the AMPT model. The $SC(2, 3)$ from the standard cumulant method is negative at a high multiplicity but changes sign towards a low multiplicity. However, the $SC(2, 3)$ from the subevent cumulant method is negative for the whole range of multiplicities. The $SC(2, 4)$ from the standard cumulant method is larger than those from the subevent cumulant methods. These results suggest that measurements based on the standard cumulant method are contaminated

by nonflow effects, and the subevent cumulant method should be used to investigate the *real* collectivity in small systems.

ACKNOWLEDGMENTS

M.-W. N. and G.-L. M. are supported by the National Natural Science Foundation of China under Grants No. 11522547, 11375251, and 11421505, and the Major State Basic Research Development Program in China under Grant No. 2014CB845404. J.J. and P.H. are supported by the National Science Foundation under Grant No. PHY-1613294.

-
- [1] J. Y. Ollitrault, *Phys. Rev. D* **46**, 229 (1992).
 [2] D. Teaney, J. Lauret, and E. V. Shuryak, *Phys. Rev. Lett.* **86**, 4783 (2001).
 [3] H. Song and U. W. Heinz, *Phys. Rev. C* **77**, 064901 (2008).
 [4] M. Luzum and P. Romatschke, *Phys. Rev. C* **78**, 034915 (2008); **79**, 039903(E) (2009).
 [5] P. Bozek, *Phys. Rev. C* **81**, 034909 (2010).
 [6] B. Schenke, S. Jeon, and C. Gale, *Phys. Rev. Lett.* **106**, 042301 (2011).
 [7] B. I. Abelev *et al.* (STAR Collaboration), *Phys. Rev. C* **80**, 064912 (2009).
 [8] B. Alver *et al.* (PHOBOS Collaboration), *Phys. Rev. Lett.* **104**, 062301 (2010).
 [9] S. Chatrchyan *et al.* (CMS Collaboration), *J. High Energy Phys.* **07** (2011) 076.
 [10] G. Aad *et al.* (ATLAS Collaboration), *Phys. Rev. C* **86**, 014907 (2012).
 [11] V. Khachatryan *et al.* (CMS Collaboration), *J. High Energy Phys.* **09** (2010) 091.
 [12] S. Chatrchyan *et al.* (CMS Collaboration), *Phys. Lett. B* **718**, 795 (2013).
 [13] B. Abelev *et al.* (ALICE Collaboration), *Phys. Lett. B* **719**, 29 (2013).
 [14] G. Aad *et al.* (ATLAS Collaboration), *Phys. Rev. Lett.* **110**, 182302 (2013).
 [15] A. Adare *et al.* (PHENIX Collaboration), *Phys. Rev. Lett.* **111**, 212301 (2013).
 [16] G. Aad *et al.* (ATLAS Collaboration), *Phys. Rev. Lett.* **116**, 172301 (2016).
 [17] G. Aad *et al.* (ATLAS Collaboration), *Phys. Rev. C* **90**, 044906 (2014).
 [18] N. Borghini, P. M. Dinh, and J. Y. Ollitrault, *Phys. Rev. C* **63**, 054906 (2001).
 [19] A. Bilandzic, R. Snellings, and S. Voloshin, *Phys. Rev. C* **83**, 044913 (2011).
 [20] J. Jia, M. Zhou, and A. Trzupek, *Phys. Rev. C* **96**, 034906 (2017).
 [21] M. Aaboud *et al.* (ATLAS Collaboration), *Phys. Rev. C* **97**, 024904 (2018).
 [22] A. Bilandzic, C. H. Christensen, K. Gulbrandsen, A. Hansen, and Y. Zhou, *Phys. Rev. C* **89**, 064904 (2014).
 [23] J. Adam *et al.* (ALICE Collaboration), *Phys. Rev. Lett.* **117**, 182301 (2016).
 [24] A. M. Sirunyan *et al.* (CMS Collaboration), *Phys. Rev. Lett.* **120**, 092301 (2018).
 [25] P. Huo, K. Gajdosov, J. Jia, and Y. Zhou, *Phys. Lett. B* **777**, 201 (2018).
 [26] P. Bozek, *Phys. Rev. C* **85**, 014911 (2012).
 [27] A. Bzdak, B. Schenke, P. Tribedy, and R. Venugopalan, *Phys. Rev. C* **87**, 064906 (2013).
 [28] E. Shuryak and I. Zahed, *Phys. Rev. C* **88**, 044915 (2013).
 [29] G.-Y. Qin and B. Müller, *Phys. Rev. C* **89**, 044902 (2014).
 [30] P. Bozek and W. Broniowski, *Phys. Rev. C* **88**, 014903 (2013).
 [31] G. L. Ma and A. Bzdak, *Phys. Lett. B* **739**, 209 (2014).
 [32] A. Bzdak and G. L. Ma, *Phys. Rev. Lett.* **113**, 252301 (2014).
 [33] J. D. Orjuela Koop, A. Adare, D. McGlinchey, and J. L. Nagle, *Phys. Rev. C* **92**, 054903 (2015).
 [34] C. Shen, J. F. Paquet, G. S. Denicol, S. Jeon, and C. Gale, *Phys. Rev. C* **95**, 014906 (2017).
 [35] R. D. Weller and P. Romatschke, *Phys. Lett. B* **774**, 351 (2017).
 [36] H. Song, Y. Zhou, and K. Gajdosova, *Nucl. Sci. Tech.* **28**, 99 (2017).
 [37] A. Dumitru, K. Dusling, F. Gelis, J. Jalilian-Marian, T. Lappi, and R. Venugopalan, *Phys. Lett. B* **697**, 21 (2011).
 [38] K. Dusling and R. Venugopalan, *Phys. Rev. D* **87**, 094034 (2013).
 [39] V. Skokov, *Phys. Rev. D* **91**, 054014 (2015).
 [40] B. Schenke, S. Schlichting, and R. Venugopalan, *Phys. Lett. B* **747**, 76 (2015).
 [41] S. Schlichting and P. Tribedy, *Adv. High Energy Phys.* **2016**, 8460349 (2016).
 [42] A. Kovner, M. Lublinsky, and V. Skokov, *Phys. Rev. D* **96**, 016010 (2017).
 [43] E. Iancu and A. H. Rezaeian, *Phys. Rev. D* **95**, 094003 (2017).
 [44] K. Dusling, W. Li, and B. Schenke, *Int. J. Mod. Phys. E* **25**, 1630002 (2016).
 [45] L. He, T. Edmonds, Z. W. Lin, F. Liu, D. Molnar, and F. Wang, *Phys. Lett. B* **753**, 506 (2016).
 [46] Z. W. Lin, L. He, T. Edmonds, F. Liu, D. Molnar, and F. Wang, *Nucl. Phys. A* **956**, 316 (2016).
 [47] Z. W. Lin, C. M. Ko, B. A. Li, B. Zhang, and S. Pal, *Phys. Rev. C* **72**, 064901 (2005).
 [48] X. N. Wang and M. Gyulassy, *Phys. Rev. D* **44**, 3501 (1991).
 [49] B. Zhang, *Comput. Phys. Commun.* **109**, 193 (1998).
 [50] B. A. Li and C. M. Ko, *Phys. Rev. C* **52**, 2037 (1995).
 [51] N. Borghini, P. M. Dinh, and J. Y. Ollitrault, *Phys. Rev. C* **64**, 054901 (2001).
 [52] S. Chatrchyan *et al.* (CMS Collaboration), *Phys. Lett. B* **724**, 213 (2013).

- [53] J. Jia and S. Radhakrishnan, *Phys. Rev. C* **92**, 024911 (2015).
- [54] L. Yan and J. Y. Ollitrault, *Phys. Rev. Lett.* **112**, 082301 (2014).
- [55] S. A. Voloshin, A. M. Poskanzer, A. Tang, and G. Wang, *Phys. Lett. B* **659**, 537 (2008).
- [56] L. Ma, G. L. Ma, and Y. G. Ma, *Phys. Rev. C* **89**, 044907 (2014).
- [57] A. Bzdak and G. L. Ma, *Phys. Rev. C* **97**, 014903 (2018).
- [58] A. Bzdak and G. L. Ma, *Phys. Lett. B* **781**, 117 (2018).